Materials Advances

ROYAL SOCIETY OF CHEMISTRY

PAPER

View Article Online
View Journal | View Issue

Cite this: *Mater. Adv.*, 2023, 4, 4755

Organic–inorganic hybrid multifunctional materials with high-T_c reversible phase transition and wide bandgap properties†

Yu-Xin Tan,[ab] Ting-Ting Ying, *[ab] Xiao-Wei Fan,[b] Yan-Le Huang,[b] Ming-Yang Wan,[b] Qiao-Lin Li,[b] Fang-Xin Wang[b] and Meng-Na Wang[b]

Received 25th July 2023,
Accepted 5th September 2023

DOI: 10.1039/d3ma00461a

rsc.li/materials-advances

Multifunctional materials play a crucial role in today's social development, but current intelligent multifunctional materials have the disadvantage of being unable to adjust their structure to meet diverse application needs. Therefore, organic–inorganic hybrid perovskites are expected to become a promising intelligent multifunctional material due to their inherent advantages in structural diversity. Here, the tetracadmium bromide inorganic material is combined with the *N*-propyl-*N*-methylpiperidine bromide organic cation to obtain a high-temperature reversible phase transition multifunctional material $[C_5H_{10}N(CH_3)CH_2CH_2CH_3]_2CdBr_4$ (**1**), which has the high-temperature reversible phase transition property of 333 K phase transition temperature, and crystallizes in the $P\bar{1}$ space group at room temperature. In addition, through UV absorption spectroscopy and first principles calculations, the optical band gap of compound **1** is 4.65 eV, indicating that the band gap of compound **1** is determined by the determination of the organic and inorganic components. This work provides ideas for discovering new high-temperature phase transition materials or researching new organic inorganic hybrid metal halide multifunctional materials.

Introduction

With the rapid development of technology, inorganic materials and organic polymer materials have also made great progress.[1–4] For example, metal halides have broad application prospects in fields such as micro nano electronics,[5] energy storage,[6,7] photocatalysis,[8] optoelectronics[9,10] and photovoltaics.[11] However, their structure cannot be adjusted as needed, which hinders their development, especially in the field of multifunctional materials. To address this issue, the functionality and flexibility of organic components, along with the excellent electronic structure and properties of inorganic components, are integrated into organic–inorganic hybrid metal halide single crystal materials.[12–14] In other words, combining the attractive characteristics of inorganic and organic systems into their structures can yield new and interesting properties.[15] Therefore, the diversity of structures and unique physical and chemical properties of organic–inorganic hybrid metal halides can provide effective solutions for the problem of the inability to adjust the structure of inorganic materials and organic polymer materials as needed. For example, $[NH_3CH_2CH_2F]_3\ BiCl_6$,[16] methylphosphonium tin triiodide $(MPSnI_3)$[17] and $(per\text{-}fluorobenzylammonium)_2PbBr_4$.[18]

As a subclass of smart material, reversible phase transition multifunctional materials can integrate multiple physical signals into one device,[19] providing new opportunities for the miniaturization of modern intelligent devices.[20] Reversible phase transition materials can respond to external signals, such as dielectric switch materials and thermochromism materials,[21] which can convert temperature signals into electrical signals and color/display signals respectively.[22] Some of them exhibit tunable dielectric behavior due to reversible structural phase transitions induced by dynamic cations.[23] The dielectric switching characteristics of such materials are very important, as they can promote the exploration and design of multifunctional materials with multiple switching response characteristics.[24–26] In particular, research on lead halide hybrid perovskite with $CH_3NH_3PbI_3$ as the marker material is very active.[27,28] Due to its unparalleled electronic and optical properties, lead halide perovskite has many fascinating application directions in solar cells, lasers, detectors, ferroelectrics, light-emitting diodes, and other fields.[29–31] As is well known, some phenomenological theories guide researchers in

[a] *Guangzhou New Life New Material Co., Ltd, Guangzhou, 510000, GuangDong Province, P. R. China. E-mail: YingTT3127@163.com*
[b] *Jiangxi Provincial Key Laboratory of Functional Molecular Materials Chemistry, Jiangxi University of Science and Technology, Ganzhou, 341000, Jiangxi Province, P. R. China*

† Electronic supplementary information (ESI) available: Experimental Sections, IR spectra, PXRD patterns, thermogravimetric graph, piezoelectric test graph, table of crystallographic data and calculation of ΔS and N. CCDC 2282715. For ESI and crystallographic data in CIF or other electronic format see DOI: https://doi.org/10.1039/d3ma00461a

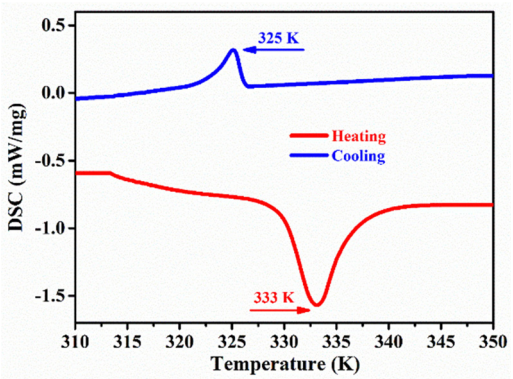

Fig. 1 The DSC curve of the heating cooling process of compound **1**.

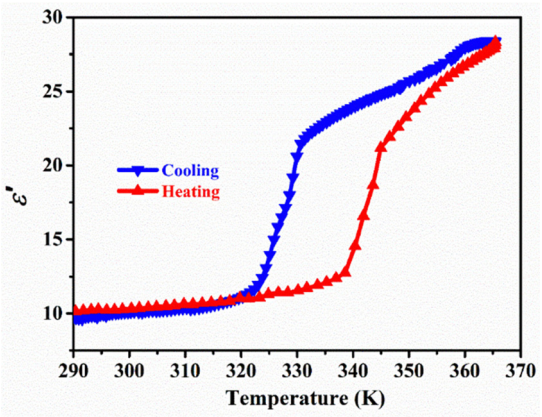

Fig. 2 The temperature heating–cooling dielectric constant diagram of compound **1**.

designing and synthesizing functional materials, such as ferroelectrics, but the relationship between structure and intrinsic properties needs further exploration.[32–34] Therefore, finding suitable inorganic materials and organic molecules and synthesizing them to obtain new organic–inorganic hybrid metal halide multifunctional materials is still an important topic for researchers.

Based on this, we successfully combined the tetra cadmium bromide inorganic material with the *N*-propyl-*N*-methylpiperidine bromide organic cation to obtain a high-temperature reversible phase transition multi-functional material: $[C_5H_{10}N(CH_3)CH_2CH_2CH_3]_2CdBr_4$ (**1**), which has the high-temperature reversible phase transition property of 333 K phase transition temperature, and crystallizes in the $P\bar{1}$ space group at room temperature. In addition, the optical band gap of compound **1** was calculated to be 4.65 eV through UV-vis absorption spectroscopy and first principles calculations, revealing that the band gap of compound **1** is synergistic between organic and inorganic components. This work has certain guiding significance for exploring more lead-free multifunctional materials with high-temperature phase transition and organic–inorganic hybrid metal halides.

Results and discussion

Slow evaporation of an aqueous solution of $CdBr_2$ and $C_5H_{10}N(CH_3)CH_2CH_2CH_3Br$ salts was performed to obtain colorless crystalline compound **1**. The presence of the organic functional group of **1** was verified through infrared spectroscopy (Fig. S1, ESI†), and its purity was confirmed through simulated PXRD and experimental PXRD curves (Fig. S2, ESI†). Thermogravimetric analysis shows that **1** is stable below 553 K, as shown by TGA in a nitrogen atmosphere (Fig. S3, ESI†). Thermal analysis (DSC) shows (Fig. 1) that there is a pair of exothermic/endothermic peaks at 333 K/325 K. Compound **1** undergoes a reversible phase transition with a phase transition temperature T_c = 333 K and a thermal hysteresis of 8 K. For convenience, we label the phases below T_c as low-temperature phases (LTP), and the phases above T_c as high-temperature phases (HTP). According to the temperature heating–cooling curve of DSC, the enthalpy transition of the phase transition process is calculated (ΔH) and the entropy change (ΔS). Using the Boltzmann equation $\Delta S = R\ln(N)$, where R is the gas constant, and the possible microstate N of **1** is 17.87 and 18.11, respectively. According to previous research, such a large N value indicates that the structural transition of compound **1** is a first-order phase transition from ordered to disordered states.

Dielectric anomaly refers to a significant change in the slope of the dielectric constant curve with temperature near T_c, which has become reliable evidence of phase transition.[35] When the static-crystal structure undergoes a dynamic transformation, it results in a sudden change in dielectric constant.[36–38] As shown in Fig. 2, there are obvious stepped dielectric anomalies during the heating and cooling processes. At the same time, the dielectric constant of the compound at 1 MHz was calculated, and the real part of the complex dielectric constant of compound **1** was calculated ε'. Starting at around 12 (LTP), there is a sharp jump that ends at 21 (HTP), maintaining a stable increase as the temperature increases. During the cooling process, the similar curve is consistent with the heating curve, with a thermal hysteresis of 8 K, corresponding to the thermal measurement curve. The reversible transition between the high and low dielectric states indicates that compound **1** undergoes a first-order reversible phase transition consistent with the DSC experimental results.[39,40]

The use of single crystal X-ray diffraction helps to understand the mechanism of thermally driven structural transformation of compounds at the microstructural level. In order to understand the structural phase transition mechanism of compound **1**, we measured the single crystal structure of compound **1** at 293 K (LTP). Under LTP, compound **1** crystallizes in the orthogonal ferroelectric space group $P\bar{1}$ (point group $\bar{1}$ with two symmetric elements (E, i)), and the unit parameters are a = 16.8749(14) Å, b = 19.2139(15) Å, c = 19.8184(15) Å, α = 118.783(2)°, β = 92.300(2)°, γ = 103.276(2)°, Z = 4 and V = 5395.1(7) Å^3. The specific cell data are shown in Table S1 (ESI†). As shown in Fig. 3a, the asymmetric unit of compound **1** in LTP consists of two $[C_5H_{10}N(CH_3)\ CH_2CH_2CH_3]^+$ cations and one $[CdBr_4]^{2-}$ tetrahedral anion, which satisfies the conservation law. At the same time, it can be seen from the stacking

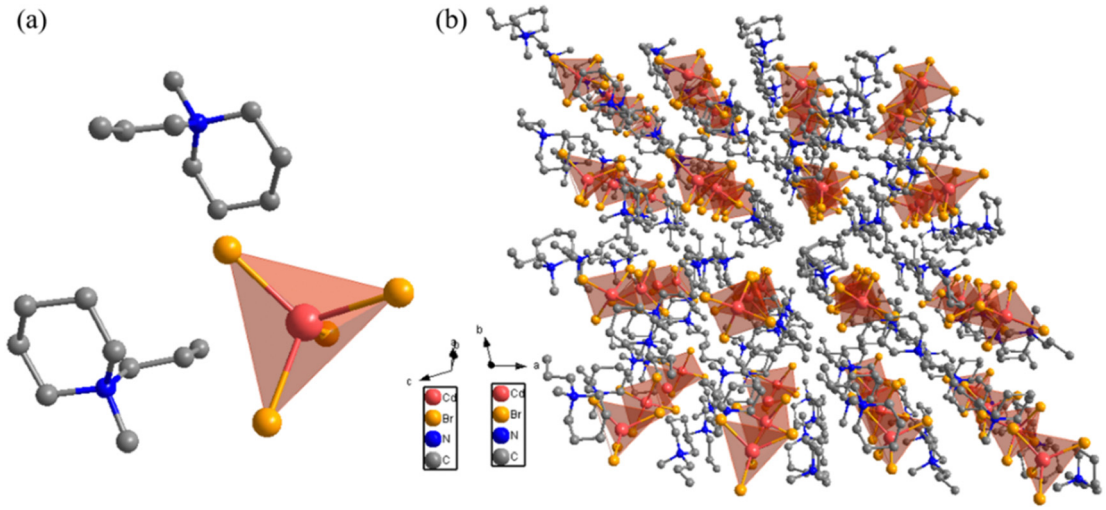

Fig. 3 (a) Asymmetric unit diagram of compound **1**. (b) Stacking diagram of compound **1**.

diagram (Fig. 3b) that compound **1** is stacked through a zero dimensional stacking method, and the organic cation $[C_5H_{10}N(CH_3)CH_2CH_2CH_3]^+$ is orderly embedded into the tetrahedron of the inorganic anion $[CdBr_4]^{2-}$, which is connected together only by intermolecular force, which provides more freedom for the movement of organic cations, leading to the occurrence of structural phase transition.[41,42]

Then, we conducted single crystal measurements at 340 K (above T_c) to detect the structure in HTP. Due to crystal quality reasons, it is difficult to determine the single crystal structure at high temperatures.[40,43,44] In addition, the slight sublimation of the crystals also led to the failure of crystal data collection. To further determine the structural phase transition, we conducted temperature dependent PXRD measurements within the range of 300 K–345 K. The experimental PXRD pattern matches well with the simulated pattern of the single crystal structure at room temperature (Fig. S2, ESI†), indicating a high crystallinity and purity of the corresponding phase. As shown in the dashed box in Fig. 4, the peaks at 17.58°, 21.19°, and 25.83°

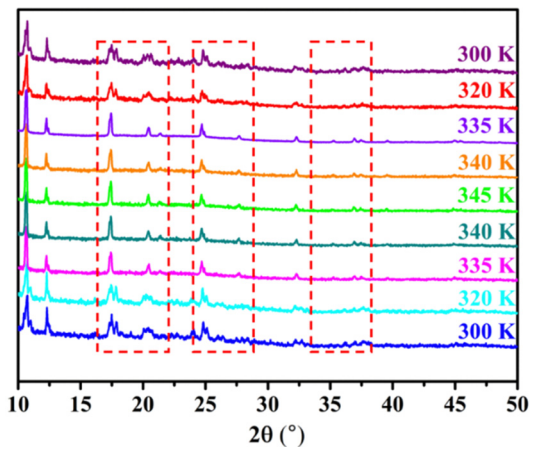

Fig. 4 Temperature dependent PXRD diagram of compound **1**.

in **1-LTP** disappear, and then reappear when returning to **1-LTP**, revealing the existence of reversible phase transition at T_c. The results are consistent with those shown in the DSC curve.

Organic compounds in organic–inorganic hybrid metal halides can affect the electronic band structure by influencing the geometric parameters of the inorganic components.[45] The dual advantages of fixed lattice and adjustable chemical composition make the configuration a promising new structural prototype with diverse and customizable optoelectronic properties.[46] As shown in the UV-vis absorption spectrum in Fig. 5a, compound **1** has a steep absorption edge at the wavelength of 239 nm, corresponding to the optical band gap of 4.65 eV derived from the *Tauc* equation (illustrated in Fig. 5a). In order to further explore the wide bandgap properties of compound **1**, the wide bandgap properties are closely related to structural assembly. The density of states of compound **1** was calculated based on first-principles theory, as shown in Fig. 5b. The PDOS plot of compound **1** shows a band gap of 3.99 eV, which is smaller than the value obtained through UV-vis spectroscopy due to theoretical limitations. In addition, it can be concluded that the conduction band of the band gap of compound **1** is affected by elements C and H, and the valence band is affected by Cd and Br, indicating that the band gap of compound **1** is jointly determined by the organic cation $[C_5H_{10}N(CH_3)CH_2CH_2CH_3]^+$ and the inorganic anion $[CdBr_4]^{2-}$. The wide bandgap properties of compound **1** provide favorable empirical evidence for the effectiveness of the combination scheme of organic and inorganic components.

Conclusions

In summary, we have successfully synthesized a new zero dimensional organic–inorganic hybrid metal halide multifunctional material: $[C_5H_{10}N(CH_3)CH_2CH_2CH_3]_2CdBr_4$ (**1**), which has the high-temperature reversible phase transition property

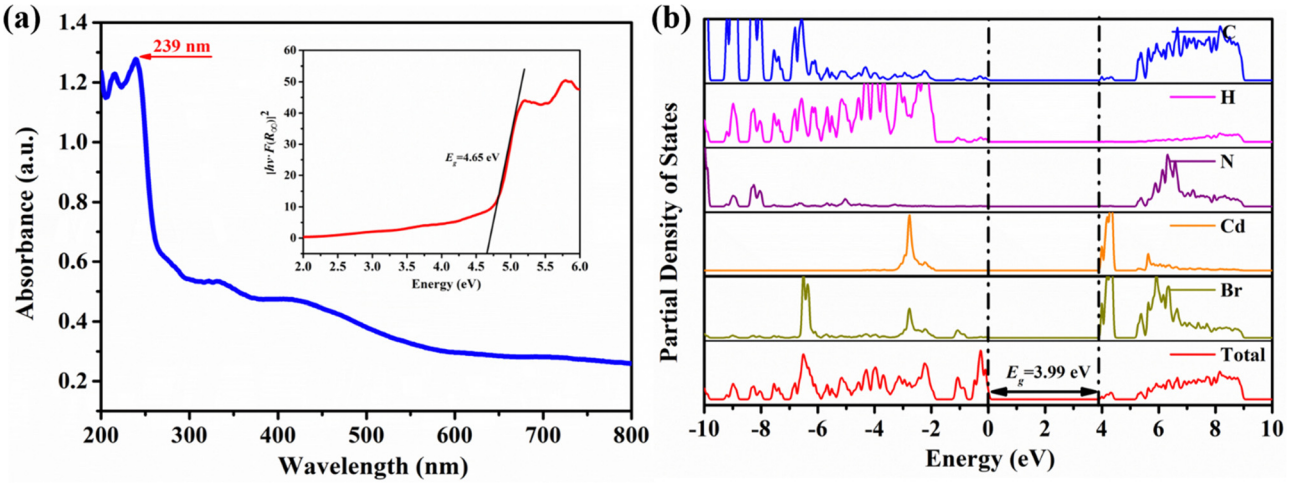

Fig. 5 (a) UV-vis absorption and optical band gap diagram of **1** calculated. (b) Partial density of states diagram of compound **1**.

at 333K phase transition temperature and crystallizes in the $P\bar{1}$ space group at room temperature. In addition, the optical band gap of compound **1** is 4.65 eV through the UV absorption spectrum and calculation, which reveals that the band gap of compound **1** is determined by organic and inorganic components. This new type of organic–inorganic hybrid metal halide high-temperature phase transition multifunctional material can promote the development of more excellent organic–inorganic hybrid multifunctional materials.

Conflicts of interest

There are no conflicts to declare.

Acknowledgements

Thanks is given for the support of the National College Students Innovation and Entrepreneurship Training Program (202210407005X) and the Key Research and Development Program of Jiangxi Province (20223BBH80010).

References

1 T. Vijayakanth, F. Ram, B. Praveenkumar, K. Shanmuganathan and R. Boomishankar, Piezoelectric Energy Harvesting from a Ferroelectric Hybrid Salt $[Ph_3MeP]_4[Ni(NCS)_6]$ Embedded in a Polymer Matrix, *Angew. Chem., Int. Ed.*, 2020, **59**, 10368–10373.

2 Y. Y. Tang, Y. L. Zeng and R. G. Xiong, Contactless Manipulation of Write-Read-Erase Data Storage in Diarylethene Ferroelectric Crystals, *J. Am. Chem. Soc.*, 2022, **144**, 8633–8640.

3 Y. Ai, R. Sun, Y. L. Zeng, J. C. Liu, Y. Y. Tang, B. W. Wang, Z. M. Wang, S. Gao and R. G. Xiong, Coexistence of magnetic and electric orderings in a divalent Cr^{2+}-based multiaxial molecular ferroelectric, *Chem. Sci.*, 2021, **12**, 9742–9747.

4 H. Xu, W. Guo, Y. Ma, Y. Liu, X. Hu, L. Hua, S. Han, X. Liu, J. Luo and Z. Sun, Record high-Tc and large practical utilization level of electric polarization in metal-free molecular antiferroelectric solid solutions, *Nat. Commun.*, 2022, **13**, 5329.

5 P. F. Li, Y. Y. Tang, Z. X. Wang, H. Y. Ye, Y. M. You and R. G. Xiong, Anomalously rotary polarization discovered in homochiral organic ferroelectrics, *Nat. Commun.*, 2016, **7**, 13635.

6 D. Lencer, M. Salinga and M. Wuttig, Design rules for phase-change materials in data storage applications, *Adv. Mater.*, 2011, **23**, 2030–2058.

7 P. F. Li, W. Q. Liao, Y. Y. Tang, H. Y. Ye, Y. Zhang and R. G. Xiong, Unprecedented Ferroelectric-Antiferroelectric-Paraelectric Phase Transitions Discovered in an Organic-Inorganic Hybrid Perovskite, *J. Am. Chem. Soc.*, 2017, **139**, 8752–8757.

8 H. Y. Zhang, Z. Wei, P. F. Li, Y. Y. Tang, W. Q. Liao, H. Y. Ye, H. Cai and R. G. Xiong, The Narrowest Band Gap Ever Observed in Molecular Ferroelectrics: Hexane-1,6-diammonium Pentaiodobismuth(III), *Angew. Chem., Int. Ed.*, 2018, **57**, 526–530.

9 X. Lu, L. Zhang, Y. Tong and Z. Y. Cheng, BST-P(VDF-CTFE) nanocomposite films with high dielectric constant, low dielectric loss, and high energy-storage density, *Composites, Part B*, 2019, **168**, 34–43.

10 Y. Wang, T. Guo, J. Yin, Z. Tian, Y. Ma, Z. Liu, Y. Zhu and H. N. Alshareef, Controlled Deposition of Zinc-Metal Anodes via Selectively Polarized Ferroelectric Polymers, *Adv. Mater.*, 2022, **34**, e2106937.

11 D. Yang, L. Luo, Y. Gao, S. Chen and X. C. Zeng, Rational design of one-dimensional hybrid organic–inorganic perovskites with room-temperature ferroelectricity and strong piezoelectricity, *Mater. Horiz.*, 2019, **6**, 1463–1473.

12 C. Xu, W. Y. Zhang, Q. Ye and D. W. Fu, Multifunctional Material with Efficient Optoelectronic Integrated Molecular Switches Based on a Flexible Thin Film/Crystal, *Inorg. Chem.*, 2017, **56**, 14477–14485.

13 B. Sun, X. F. Liu, X. Y. Li, Y. Cao, Z. Yan, L. Fu, N. Tang, Q. Wang, X. Shao, D. Yang and H. L. Zhang, Reversible

Thermochromism and Strong Ferromagnetism in Two-Dimensional Hybrid Perovskites, *Angew. Chem., Int. Ed.*, 2020, **59**, 203–208.

14 M. J. Yang, S. Y. Tang, Y. R. Weng, F. Zhou, Y. Shi, Y. J. Bai and Y. Ai, H/F Substitution on the Spacer Cations Leads to 1D-to-2D Increment of the Pyrrolidinium-Containing Lead Iodide Hybrid Perovskites, *Inorg. Chem.*, 2022, **61**, 5836–5843.

15 C. F. Wang, C. Shi, A. Zheng, Y. Wu, L. Ye, N. Wang, H. Y. Ye, M. G. Ju, P. Duan, J. Wang and Y. Zhang, Achieving circularly polarized luminescence and large piezoelectric response in hybrid rare-earth double perovskite by a chirality induction strategy, *Mater. Horiz.*, 2022, **9**, 2450–2459.

16 L.-L. Chu, T. Zhang, Y.-F. Gao, W.-Y. Zhang, P.-P. Shi, Q. Ye and D.-W. Fu, Fluorine Substitution in Ethylamine Triggers Second Harmonic Generation in Noncentrosymmetric Crystalline $[NH_3CH_2CH_2F]_3BiCl_6$, *Chem. Mater.*, 2020, **32**, 6968–6974.

17 H. Y. Zhang and R. G. Xiong, Three-dimensional narrow-bandgap perovskite semiconductor ferroelectric methylphosphonium tin triiodide for potential photovoltaic application, *Chem. Commun.*, 2023, **59**, 920–923.

18 H. Y. Zhang, Z. X. Zhang, X. J. Song, X. G. Chen and R. G. Xiong, Two-Dimensional Hybrid Perovskite Ferroelectric Induced by Perfluorinated Substitution, *J. Am. Chem. Soc.*, 2020, **142**, 20208–20215.

19 H. Y. Ye, Q. Zhou, X. Niu, W. Q. Liao, D. W. Fu, Y. Zhang, Y. M. You, J. Wang, Z. N. Chen and R. G. Xiong, High-Temperature Ferroelectricity and Photoluminescence in a Hybrid Organic-Inorganic Compound: (3-Pyrrolinium) $MnCl_3$, *J. Am. Chem. Soc.*, 2015, **137**, 13148–13154.

20 C. Shi, L. Ye, Z. X. Gong, J. J. Ma, Q. W. Wang, J. Y. Jiang, M. M. Hua, C. F. Wang, H. Yu, Y. Zhang and H. Y. Ye, Two-Dimensional Organic-Inorganic Hybrid Rare-Earth Double Perovskite Ferroelectrics, *J. Am. Chem. Soc.*, 2020, **142**, 545–551.

21 R. G. Xiong, S. Q. Lu, Z. X. Zhang, H. Cheng, P. F. Li and W. Q. Liao, A Chiral Thermochromic Ferroelastic with Seven Physical Channel Switches, *Angew. Chem., Int. Ed.*, 2020, **59**, 9574–9578.

22 B. Huang, L. Y. Sun, S. S. Wang, J. Y. Zhang, C. M. Ji, J. H. Luo, W. X. Zhang and X. M. Chen, A near-room-temperature organic-inorganic hybrid ferroelectric: $[C_6H_5CH_2CH_2NH_3]_2[CdI_4]$, *Chem. Commun.*, 2017, **53**, 5764–5766.

23 T.-T. Ying, Y.-Z. Tang, Y.-H. Tan, J.-Y. Wang, Y.-R. Zhao, X.-W. Fan, F.-X. Wang and M.-Y. Wan, A novel Cd-based multifunctional high temperature phase transition material: $[(CH_2CH_3)_3NCH_2Cl]_2CdBr_4$, *Inorg. Chim. Acta*, 2023, **545**, 121254.

24 C. Zhou, H. Lin, Y. Tian, Z. Yuan, R. Clark, B. Chen, L. J. van de Burgt, J. C. Wang, Y. Zhou, K. Hanson, Q. J. Meisner, J. Neu, T. Besara, T. Siegrist, E. Lambers, P. Djurovich and B. Ma, Luminescent zero-dimensional organic metal halide hybrids with near-unity quantum efficiency, *Chem. Sci.*, 2018, **9**, 586–593.

25 H. Y. Zhang, Y. Y. Tang, P. P. Shi and R. G. Xiong, Toward the Targeted Design of Molecular Ferroelectrics: Modifying Molecular Symmetries and Homochirality, *Acc. Chem. Res.*, 2019, **52**, 1928–1938.

26 C. K. Yang, W. N. Chen, Y. T. Ding, J. Wang, Y. Rao, W. Q. Liao, Y. Xie, W. Zou and R. G. Xiong, Directional Intermolecular Interactions for Precise Molecular Design of a High-Tc Multiaxial Molecular Ferroelectric, *J. Am. Chem. Soc.*, 2019, **141**, 1781–1787.

27 J. Y. Jiang, Q. Xu, J. J. Ma, Z. X. Gong, C. Shi and Y. Zhang, Above room-temperature dielectric switching and semiconducting properties of a layered organic-inorganic hybrid compound: (C(6)H(12)N)(2)Pb(NO(3))(4), *Dalton Trans.*, 2020, **49**, 16860–16865.

28 Q. Pan, Z. B. Liu, Y. Y. Tang, P. F. Li, R. W. Ma, R. Y. Wei, Y. Zhang, Y. M. You, H. Y. Ye and R. G. Xiong, A Three-Dimensional Molecular Perovskite Ferroelectric: (3-Ammoniopyrrolidinium)$RbBr_3$, *J. Am. Chem. Soc.*, 2017, **139**, 3954–3957.

29 R. K. Saripalli, D. Swain, S. Prasad, H. Nhalil, H. L. Bhat, T. N. Guru Row and S. Elizabeth, Observation of ferroelectric phase and large spontaneous electric polarization in organic salt of diisopropylammonium iodide, *J. Appl. Phys.*, 2017, **121**, 114101.

30 H. Y. Ye, W. Q. Liao, C. L. Hu, Y. Zhang, Y. M. You, J. G. Mao, P. F. Li and R. G. Xiong, Bandgap Engineering of Lead-Halide Perovskite-Type Ferroelectrics, *Adv. Mater.*, 2016, **28**, 2579–2586.

31 S. Wang, X. Liu, L. Li, C. Ji, Z. Sun, Z. Wu, M. Hong and J. Luo, An Unprecedented Biaxial Trilayered Hybrid Perovskite Ferroelectric with Directionally Tunable Photovoltaic Effects, *J. Am. Chem. Soc.*, 2019, **141**, 7693–7697.

32 P. P. Shi, Y. Y. Tang, P. F. Li, W. Q. Liao, Z. X. Wang, Q. Ye and R. G. Xiong, Symmetry breaking in molecular ferroelectrics, *Chem. Soc. Rev.*, 2016, **45**, 3811–3827.

33 W. Zhang and R. G. Xiong, Ferroelectric metal-organic frameworks, *Chem. Rev.*, 2012, **112**, 1163–1195.

34 K. Yang, X.-X. Dong, Q. Xu, Y.-H. Tan and Y.-Z. Tang, Nopinic acid is an unprecedented homochiral single-component organic ferroelectric, *Appl. Mater. Today*, 2020, **20**, 100687.

35 W. J. Xu, P. F. Li, Y. Y. Tang, W. X. Zhang, R. G. Xiong and X. M. Chen, A Molecular Perovskite with Switchable Coordination Bonds for High-Temperature Multiaxial Ferroelectrics, *J. Am. Chem. Soc.*, 2017, **139**, 6369–6375.

36 Y. Sui, Y.-S. Zhong, J.-J. Wang, Q. Xia, L.-J. Wang and D.-S. Liu, A semiconducting organic–inorganic hybrid $([BrCH_2CH_2N(CH_3)_3]^{2+}[CuBr_4]^{2-})$ with switchable dielectric properties derived from an unusual piston-like displacive movement, *J. Mater. Chem. C*, 2019, **7**, 14294–14300.

37 T. Ying, Y. Li, N. Song, Y. Tan, Y. Tang, J. Zhuang, H. Zhang and L. Wang, Semi-conductive, Switchable Dielectric and Photoluminescent Properties of Two High-Temperature Phase Transition Hybrids, *Chem. – Asian J.*, 2021, **16**, 3664–3668.

38 N. Song, X. X. Dong, J. C. Zhuang, Y. K. Li, D. C. Han, Y. H. Tan, W. J. Wei and Y. Z. Tang, Coupling Narrow Band Gap and Switchable SHG Responses in a New Molecule Ferroelectric: Imidazolyl Propylamine Pentabromo Stibium(III), *Inorg. Chem.*, 2021, **60**, 1195–1201.

39 Q.-Q. Jia, Q.-F. Luo, H.-F. Ni, C.-Y. Su, D.-W. Fu, L.-Y. Xie and H.-F. Lu, High-Sensitivity Organic–Inorganic Hybrid Materials with Reversible Thermochromic Property and Dielectric Switching, *J. Phys. Chem. C*, 2022, **126**, 1552–1557.

40 T.-T. Ying, Y.-Z. Tang, Y.-H. Tan, Y.-R. Zhao, J.-Y. Wang, M.-Y. Wan, F. X. Wang, X. W. Fan and Y. K. Li, Organic Single-Component Enantiomers with High Phase Transition Temperatures and Dielectric Switching Properties, *Cryst. Growth Des.*, 2022, **22**, 7501–7507.

41 J. Harada, T. Shimojo, H. Oyamaguchi, H. Hasegawa, Y. Takahashi, K. Satomi, Y. Suzuki, J. Kawamata and T. Inabe, Directionally tunable and mechanically deformable ferroelectric crystals from rotating polar globular ionic molecules, *Nat. Chem.*, 2016, **8**, 946–952.

42 C. Ji, S. Wang, L. Li, Z. Sun, M. Hong and J. Luo, The First 2D Hybrid Perovskite Ferroelectric Showing Broadband White–Light Emission with High Color Rendering Index, *Adv. Funct. Mater.*, 2018, **29**, 1805038.

43 T. Ying, Y. Tan, Y. Tang, X. Fan, F. Wang, M. Wan, J. Liao and Y. Huang, High-Tc Quadratic Nonlinear Optical and Dielectric Switchings in Fe-Based Plastic Crystalline Ferroelectric, *Inorg. Chem.*, 2022, **61**, 20608–20615.

44 Y. Ai, P. F. Li, M. J. Yang, Y. Q. Xu, M. Z. Li and R. G. Xiong, An organic plastic ferroelectric with high Curie point, *Chem. Sci.*, 2022, **13**, 748–753.

45 H. Y. Zhang, H. H. Jiang, Y. Zhang, N. Zhang and R. G. Xiong, Ferroelectric Lithography in Single-Component Organic Enantiomorphic Ferroelectrics, *Angew. Chem., Int. Ed.*, 2022, **61**, e202200135.

46 D. Fu, J. Xin, Y. He, S. Wu, X. Zhang, X. M. Zhang and J. Luo, Chirality-Dependent Second-Order Nonlinear Optical Effect in 1D Organic-Inorganic Hybrid Perovskite Bulk Single Crystal, *Angew. Chem., Int. Ed.*, 2021, **60**, 20021–20026.